CIB-W18/40-7-2

INTERNATIONAL COUNCIL FOR RESEARCH AND INNOVATION
IN BUILDING AND CONSTRUCTION

WORKING COMMISSION W18 - TIMBER STRUCTURES

EDGE JOINTS WITH DOWEL TYPE FASTENERS IN CROSS LAMINATED TIMBER

T Uibel
H J Blaß

Universität Karlsruhe

Germany

MEETING FORTY
BLED
SLOVENIA
AUGUST 2007

Edge Joints with Dowel Type Fasteners in Cross Laminated Timber

T. Uibel, H.J. Blaß
Lehrstuhl für Ingenieurholzbau und Baukonstruktionen
Universität Karlsruhe, Germany

1 Introduction

During the 39th meeting of CIB-W18 the authors presented proposals for the calculation of the load carrying capacity of joints with dowel type fasteners positioned perpendicular to the plane of cross laminated timber (CLT) [4]. In continuation of the research project [1] the load carrying capacity of edge joints with dowels and screws in CLT was examined. To calculate the load carrying capacity of dowel-type fasteners according to Johansen's yield theory [2], [3] the yield moment of the fasteners and the embedding strength are needed. The withdrawal strength is necessary to calculate the load carrying capacity of axially loaded screws. In addition, the withdrawal strength is important for estimating the rope effect of laterally loaded connections. In the narrow sides of CLT the fasteners can be positioned parallel to the grain direction. The embedment strength and the withdrawal strength are also influenced by gaps and grooves.

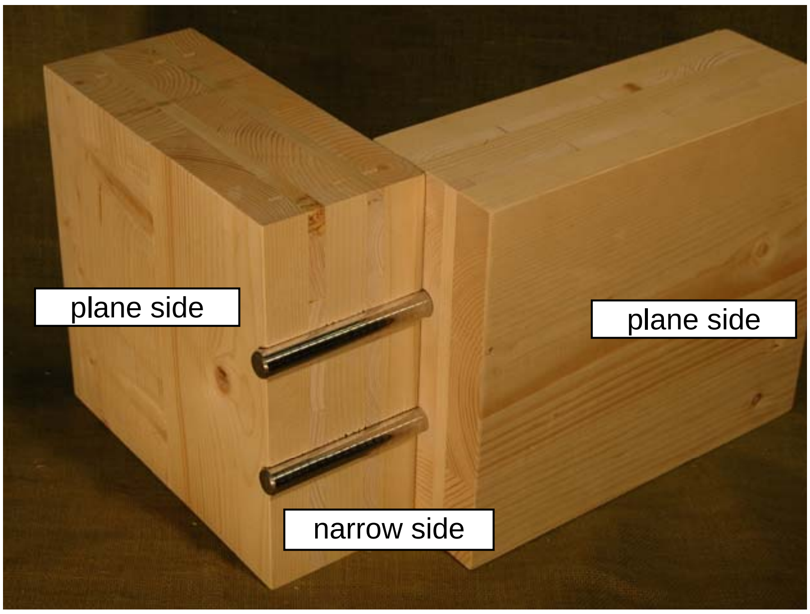

Fig. 1: Opened connection with dowels in cross laminated timber

2 Embedding strength

2.1 Test set-up and test material

The embedment tests with dowels, screws and nails in CLT were carried out according to EN 383 [5]. To avoid splitting of test specimens tensile reinforcements were required in some cases. For this purpose stripes of plywood were glued onto the surface of the test specimen, as shown in Fig. 2. The stripes were placed in some distance to the fastener to exclude influences on the embedment strength and on the stress distribution within close range of the fastener.

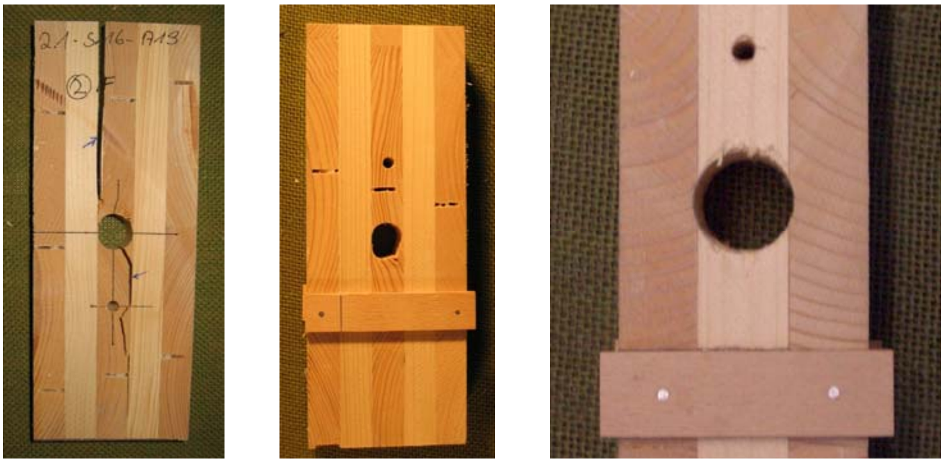

Fig. 2: Splitting failure of test specimen and tensile reinforcements to avoid splitting

The test programme includes tests with two different load directions as shown in Fig. 3 (direction A and B). In the narrow sides of CLT many positions of fasteners are possible. Fig. 4 shows five possible positions of fasteners with different diameters in relation to the thickness of the layers and in relation to the grain direction. The examined positions of fasteners in relation to gaps and grooves are displayed in Fig. 5. It was not possible to determine the relevant configuration before the tests. Thirteen different combinations of load direction and fastener positions were considered in the tests with dowels while in the tests with screws and nails seven combinations were included.

For the tests CLT made of European spruce (*Picea abies*) from four different manufacturers with seven different build-ups were used. Table 1 gives some statistical information about the density of the test specimens.

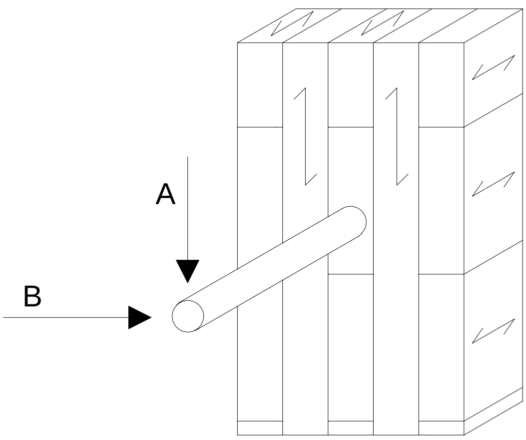

Fig. 3: Tested load directions, schematic sketch of a test specimen

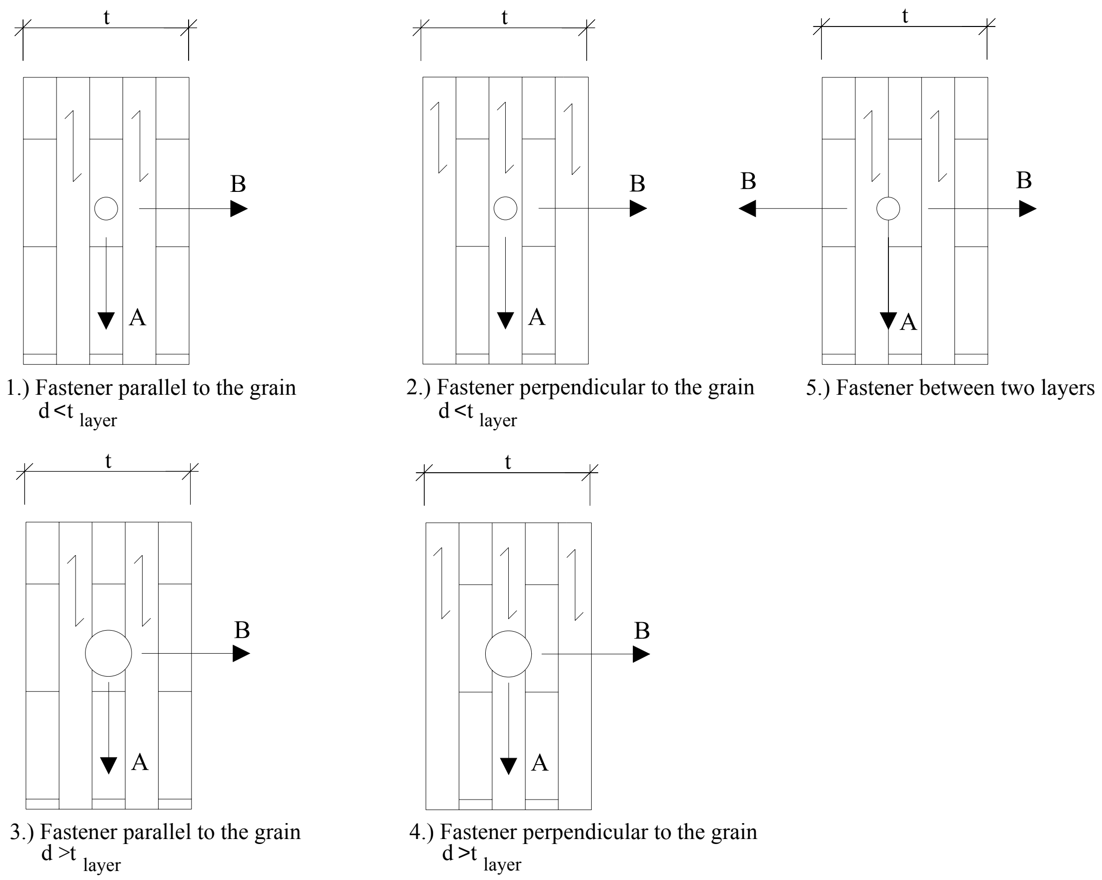

Fig. 4: Possible positions of fasteners in the narrow sides, schematic sketch

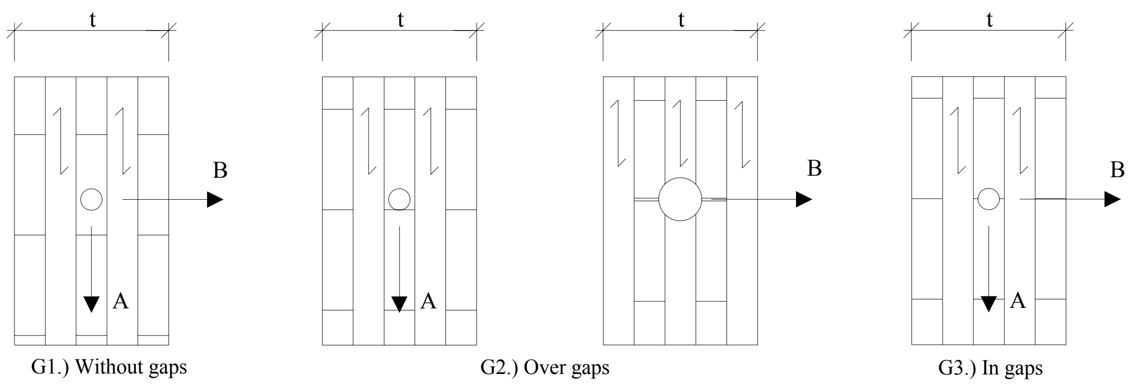

Fig. 5: Possible positions of the fasteners in relation to gaps, schematic sketch

Table 1: Density of the specimens at normal climate, 20°C/65% RH

Manufacturer/ product	n	Density of the whole cross section			Density of the relevant layers		
		ρ_{mean} kg/m³	Coefficient of variation	$\rho_{0,05}$ kg/m³	ρ_{mean} kg/m³	Coefficient of variation	$\rho_{0,05}$ kg/m³
1	184	474	5,76 %	434	481	9,54 %	412
2	292	439	7,65 %	391	417	12,2 %	345
3, 4	233	452	5,55 %	413	461	9,89 %	401

2.2 Results for dowels

To determine the embedding strength of cross laminated timber 390 tests with dowels were evaluated. For the tests dowels with 24, 16, 12, 8 and 6 mm in diameter were used. The test results in the different test configurations were analysed to reveal the relevant position.
Fig. 6 shows the ratio $f_{h,test}/\rho$ over the diameter for the tested dowel positions. The test configurations are named after the combination of load direction (A, B as shown in Fig. 3) and the position of the fasteners (1 to 5 as shown in Fig. 4). The tests carried out in position A1 result in the lowest values for the embedment strength.

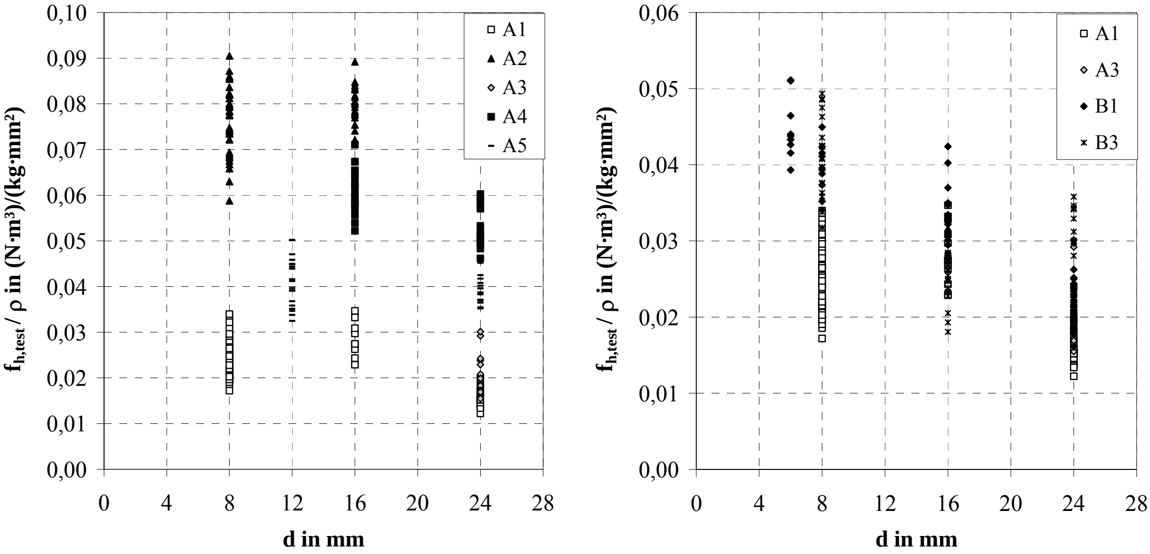

Fig. 6: Ratio $f_{h,test}/\rho$ over diameter d for the different tested positions of dowels

For dowels it was possible to develop the model for the embedment strength given in equation (1). It is based on a multiple regression analysis of 100 embedment tests carried out in the relevant test position A1. The embedment strength depends on the diameter d of the dowel and the density ρ_{layer} of the layer or the layers in which the dowel is placed.

$$f_{h,pred} = 0{,}049 \cdot (1 - 0{,}017 \cdot d) \cdot \rho_{layer}^{0{,}91} \qquad \text{in N/mm}^2 \qquad (1)$$

$$r = 0{,}63$$

with

d diameter of the fastener

ρ_{layer} density of the relevant layer(s)

A comparison of predicted values and test results is shown in Fig. 7. The correlation coefficient r is equal to 0,63. The diagram shows also the results for the non-relevant positions. By inserting the characteristic density of the relevant layer which complies with the density of the raw material (350 kg/m³ for C24) in equation (1) the characteristic embedment strength can be proposed as:

$$f_{h,k} = 0{,}0435 \cdot \left(1 - 0{,}017 \cdot d\right) \cdot \rho_{layer,k}^{0{,}91} = 9 \cdot \left(1 - 0{,}017 \cdot d\right) \qquad \text{in N/mm}^2 \qquad (2)$$

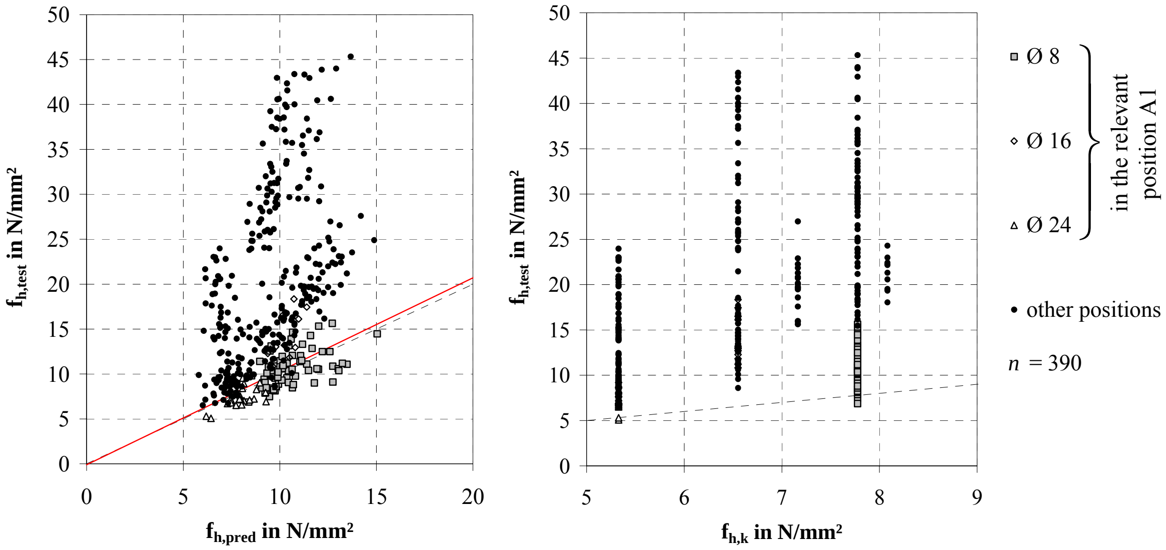

Fig. 7: Comparison of test results and predicted values resp. characteristic values of the embedment strength, influence of the dowel position

2.3 Results for screws and nails

Altogether 319 embedment tests with nails (d = 4,2 mm) and screws (d = 6, 8, 12 mm) in seven different combinations of load direction and fastener positions were carried out. On the basis of a regression analysis of 117 tests with screws and nails in the relevant test configuration A1 the embedment strength can be derived as:

$$f_{h,pred} = 0{,}8622 \cdot d^{-0{,}46} \cdot \rho_{layer}^{0{,}56} \qquad \text{in N/mm}^2 \qquad (3)$$

$$r = 0{,}68$$

A comparison of predicted values and test results is shown in Fig. 8. The correlation coefficient was determined as r = 0,68. Having inserted the characteristic density of the layers ($\rho_{layer,k}$ = 350 kg/m³) in (3), simplified and adapted the equation the characteristic embedment strength can be proposed as:

$$f_{h,k} = 0{,}862 \cdot d^{-0{,}5} \cdot \rho_{layer,k}^{0{,}56} = 20 \cdot d^{-0{,}5} \qquad \text{in N/mm}^2 \qquad (4)$$

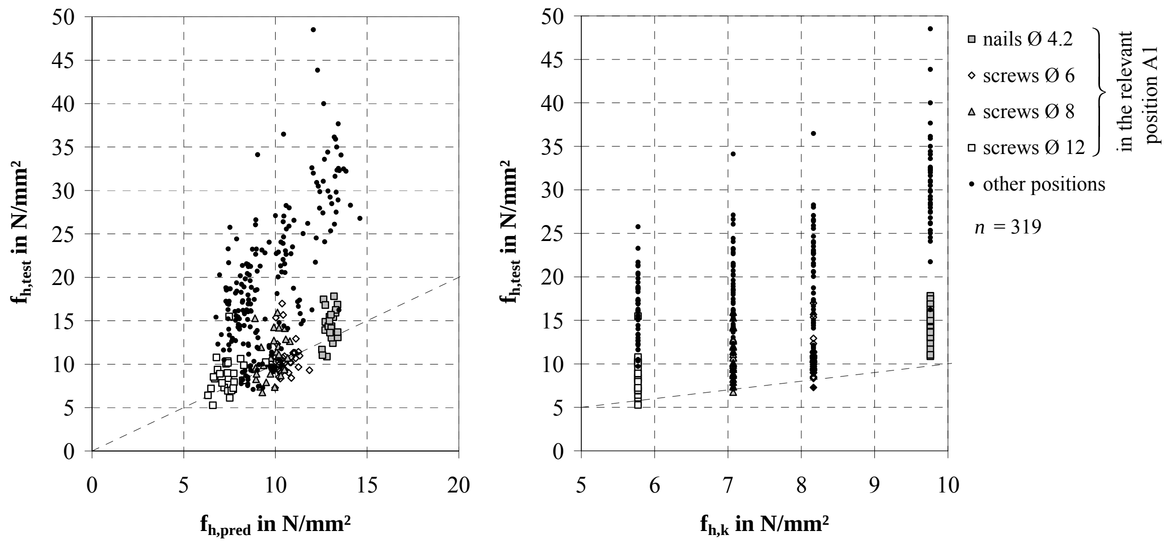

Fig. 8: Comparison of test results and predicted or characteristic values (screws/nails) resp.

3 Withdrawal strength of self-tapping screws in CLT

3.1 Test set-up and test material

To determine the withdrawal strength of self-tapping screws in CLT 119 tests with screws placed perpendicular to the plane of CLT and 268 tests with screws in the edges of CLT were carried out according to EN 1382 [6]. In the tests the positions of screws were varied, as shown in Fig. 9 and 10. In the plane side they were positioned in areas without gaps (position 1.1) and placed in gaps (position 1.2 to 1.4). Screws driven perpendicular (position C) and parallel (positions A, B) to the grain were considered in the edge withdrawal tests. Furthermore, tests with screws placed in gaps (positions B.1, B.2) were taken into consideration to derive the withdrawal capacity. Table 3 shows the statistical summary of the specimen density.

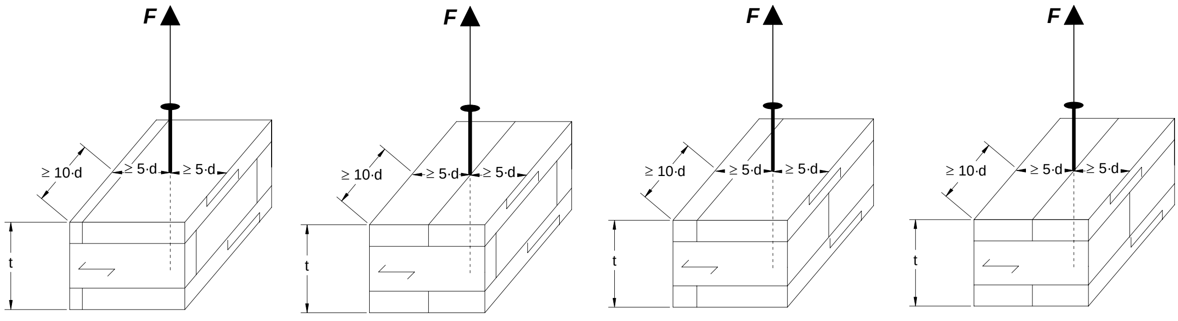

Position 1.1 1.2 1.3 1.4

Fig. 9: Set-up for withdrawal tests with screws positioned perp. to the plane of CLT

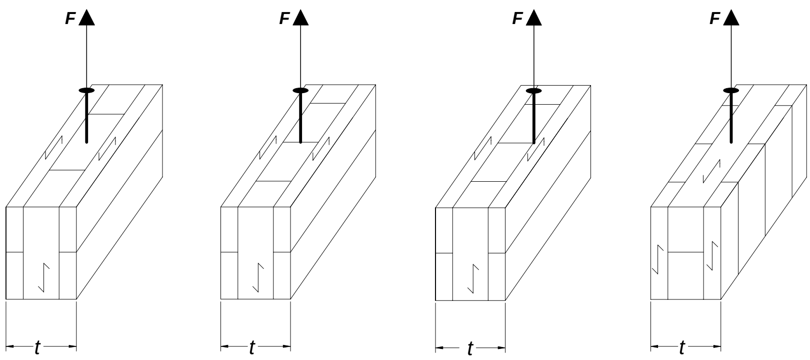

Position A B.1 B.2 C

Fig. 10: Set-up for edge withdrawal tests with screws in CLT

Table 2: Density of the specimens at normal climate, 20°C/65% RH

Manufacturer/ product	Density of the specimen for withdrawal tests							
	Plane side (hole cross section)				Narrow side (relevant layers)			
	n	ρ_{mean} kg/m³	Coefficient of variation	$\rho_{0,05}$ kg/m³	n	ρ_{mean} kg/m³	Coefficient of variation	$\rho_{0,05}$ kg/m³
1	24	454	4,48 %	423	57	448	8,21 %	374
2	73	426	5,44 %	384	159	404	11,9 %	335
3, 4	22	445	3,34 %	420	52	435	8,29 %	382

3.2 Test results

The best correlation between test results and predicted values can be achieved if the withdrawal capacity of self-tapping screws in CLT is calculated according to the following expression:

$$R_{ax,s,pred} = \frac{0,44 \cdot d^{0,8} \cdot \ell_{ef}^{0,9} \cdot \rho^{0,75}}{1,25 \cdot \cos^2\varepsilon + \sin^2\varepsilon} \quad \text{in N} \qquad (5)$$

$r = 0,91$

with

d nominal or outer diameter of the screw in mm

ℓ_{ef} effective pointside penetration length in mm

ε angle between screw axis and grain direction

ρ for joints in the plane side of CLT: density of CLT (whole cross section) in kg/m³
for edge joints in CLT: density of the relevant layer(s) in kg/m³

Fig. 11 (left) shows the test results vs. the predicted values. The correlation coefficient r is equal to 0,91. To simplify equation (5) the characteristic density of CLT is inserted and the denominator is increased up to 1,5. A further adaptation results in equation (6) for the characteristic withdrawal capacity. The right diagram in Fig. 11 shows the verification of the characteristic values.

$$R_{ax,s,k} = \frac{0,35 \cdot d^{0,8} \cdot \ell_{ef}^{0,9} \cdot \rho^{0,75}}{1,5 \cdot \cos^2\varepsilon + \sin^2\varepsilon} = \frac{31 \cdot d^{0,8} \cdot \ell_{ef}^{0,9}}{1,5 \cdot \cos^2\varepsilon + \sin^2\varepsilon} \quad \text{in N} \qquad (6)$$

with

ε joints in the plane side of CLT: $\varepsilon = 90°$, edge joints: $\varepsilon = 0°$

ρ characteristic density of CLT (400 kg/m³)

The given equations are only valid for self-tapping screws, for which the characteristic withdrawal strength in solid wood (C24) exceeds $f_{ax,k} = 80 \cdot \rho_k^2 \cdot 10^{-6} = 9,8$ N/mm².

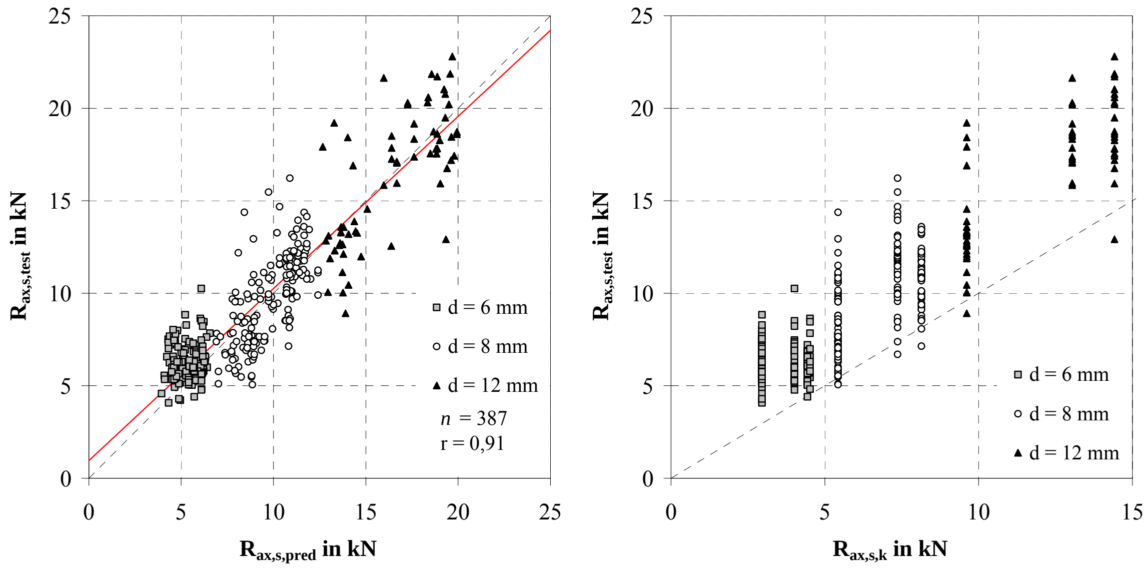

Fig. 11: Withdrawal strength - test results over predicted or characteristic values resp.

4 Load carrying capacity of edge joints

4.1 Short-term tests

In order to confirm the calculation of the load carrying capacities of edge joints in CLT 49 tests with dowels and screws were carried out. The tests also provide a basis for determining the required spacing, edge and end distances for the fasteners, which are defined in Fig. 14. Table 3 shows the specimen parameters while table 4 shows the results of the tests. Connections with fasteners placed parallel to the grain (configuration B) and perpendicular to the grain (configuration A) were considered in the tests. Furthermore, joints with fasteners placed between two layers of different grain direction were tested in configuration C. Comparisons between test results and calculated load carrying capacities are given in Fig. 12 and Fig. 13.

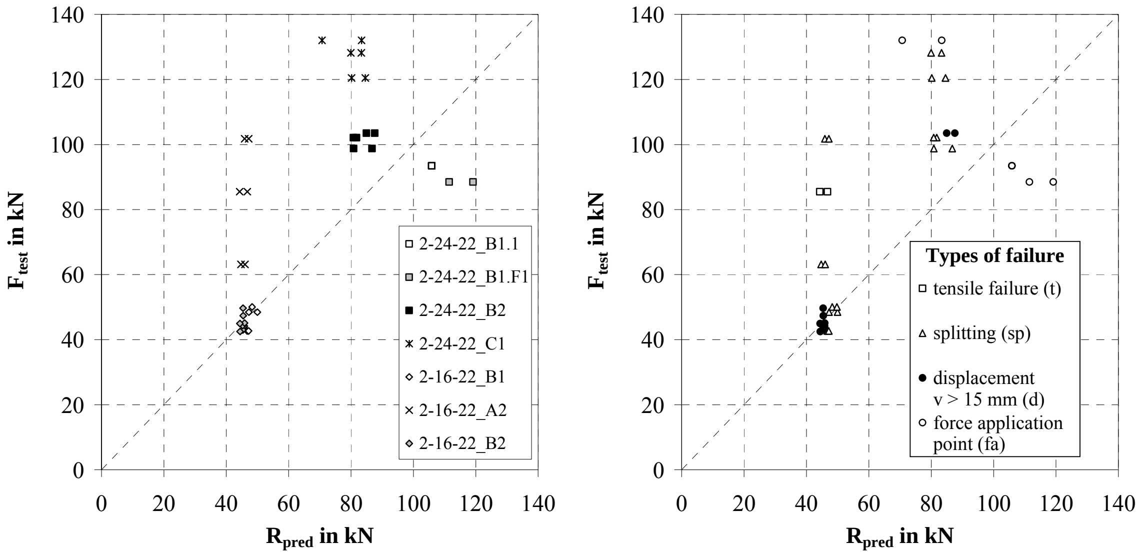

Fig. 12: Test results for edge joints with dowels vs. predicted load carrying capacities

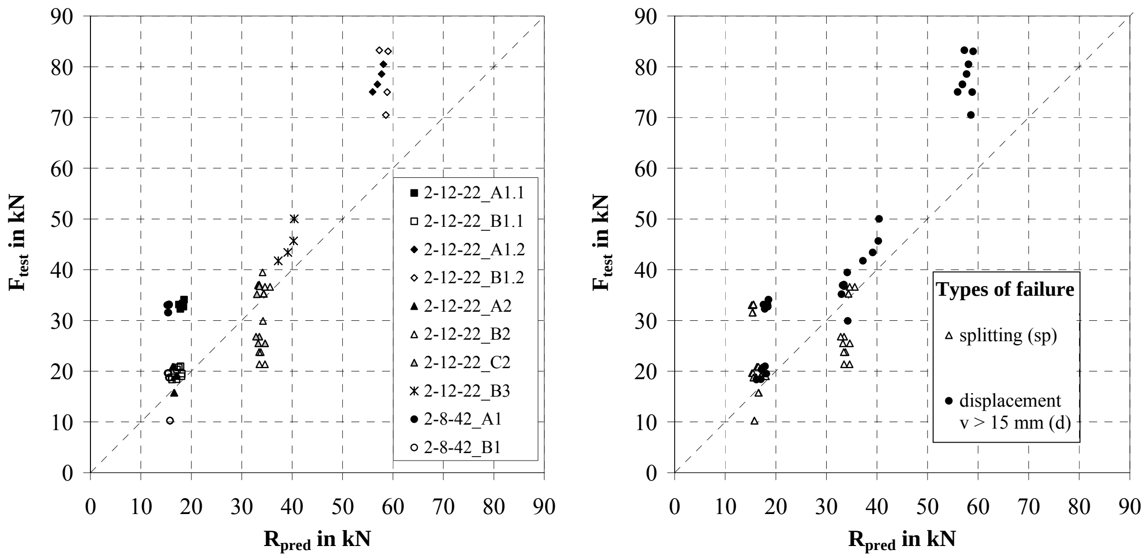

Fig. 13: Test results for edge joints with screws vs. predicted load carrying capacities

Table 3: Specimen parameters

Specimen	n_{test}	Conf.	Fasteners											Build-up of CLT
			Type	d mm	M_y Nm	t_1 mm	t_2 mm	$a_{3,t}$ mm	a_1 mm	$a_{4,c}$ mm	s	m	n	Side and middle members
2-24-22_B1	1	B	dowels	24	1224	96	160	5·d	4·d	64	2	1	5	34-13-34-13-34
2-24-22_B1.F1	1	B	dowels	24	1224	96	160	5·d	4·d	64	2	1	4	34-13-34-13-34
2-24-22_C1	3	C	dowels	24	1224	96	160	5·d	4·d	89	2	1	3	34-22-34-22-34-22-34 (reduced to 178 mm)
2-24-22_B2	3	B	dowels	24	1224	96	160	5·d	4·d	101	2	1	3	34-22-34-22-34-22-34
2-16-22_B1	3	B	dowels	16	400	80	160	5·d	4·d	30	2	1	3	19-22-19
2-16-22_A2	3	A	dowels	16	400	80	160	5·d	5·d	64	2	1	3	34-13-34-13-34
2-16-22_B2	4	B	dowels	16	400	80	160	5·d	5·d	64	2	1	3	34-13-34-13-34
2-12-22_A1.1	3	A	screws	12	63,7[1]/100,8[2]	120	120	12·d	10·d	64	1	1	2	34-13-34-13-34
2-12-22_B1.1	4	B	screws	12	63,7[1]/100,8[2]	60	120	12·d	4·d	30	2	1	2	19-22-19
2-12-22_A1.2	2	A/B	screws	12	63,7[1]/100,8[2]	120	120	12·d	10·d	36,5	1	3	2	34-22-34-22-34
2-12-22_B1.2	2	B/A	screws	12	63,7[1]/100,8[2]	120	120	12·d	10·d	36,5	1	3	2	34-22-34-22-34
2-12-22_A2	3	A	screws	12	63,7[1]/100,8[2]	60	120	7·d	4·d	64	2	1	2	34-13-34-13-34
2-12-22_B2	6	B	screws	12	63,7[1]/100,8[2]	60	120	7·d	4·d	30	2	1	4	19-22-19
2-12-22_C2	3	C	screws	12	63,7[1]/100,8[2]	60	120	7·d	4·d	48	2	1	4	34-13-34-13-34 (reduced to 96 mm)
2-12-22_B3	2	B	screws	12	63,7[1]/100,8[2]	120	120	10·d	5·d	30	1	1	4	19-22-19
2-8-42_A1	3	A	screws	8	24,1	120	80	10·d	7·d	21	1	1	2	8,5-7,5-10-7,5-8,5
2-8-42_B1	3	B	screws	8	24,1	80	120	7·d	5·d	21	1	1	2	8,5-7,5-10-7,5-8,5
s: Number of shear planes per fastener; m: Number of fastener rows; n: Number of fasteners per row; 1) Yield moment of the thread of the screw; 2) Yield moment of the shank of the screw														

Table 4: Results of the tests

Specimen	Number of specimens n	Mean density $\rho_{layer,m}$ in kg/m³		Load carrying capacity per fastener and shear plane $F_{u,mean}$ in kN	Type of failure
		Side members	Middle members		
2-24-22_B1	1	408	410	9,35	1 x fa
2-24-22_B1.F1	1	405	355	11,1	1 x fa
2-24-22_C1	3	441	416	21,2	1 x fa, 2 x sp
2-24-22_B2	3	456	449	16,9	2 x d, 1 x sp+d
2-16-22_B1	3	451	482	7,85	3 x sp
2-16-22_A2	3	438	391	13,9	2 x sp, 1 x t
2-16-22_B2	4	397	433	7,52	4 x d
2-12-22_A1.1	3	400	399	8,28	3 x d
2-12-22_B1.1	4	464	442	4,88	4 x d
2-12-22_A1.2	2	431	392	6,47	2 x d
2-12-22_B1.2	2	436	446	6,50	2 x d
2-12-22_A2	3	430	388	4,64	3 x sp
2-12-22_B2	6	449	428	3,93	2 x sp, 2 x d 2 x sp+d
2-12-22_C2	3	428	428	3,68	2 x sp, 1 x d
2-12-22_B3	2	439	439	5,65	2 x d
2-8-42_A1	3	474	492	8,15	3 x sp
2-8-42_B1	3	477	518	4,06	3 x sp
fa: failure at the force application point; sp: splitting of the layers; d: displacement v >15 mm; t: tensile failure					

For most of the test series with fasteners placed parallel to the grain (configuration B) the calculated loads and the test results correspond. In the other configurations the load carrying capacity is underestimated. The reason for this discrepancy is the conservatively assumed embedment strength, which also has to cover fasteners positioned parallel to the grain. Besides, differences between the calculated load carrying capacity and the test results are determined for connections with small spacings and end distances. In these tests splitting occurred. To avoid this failure the requirements given in Fig. 14 and Table 5 have to be fulfilled. For the design of multiple fastener joints it is suggested to consider the effective number of fasteners.

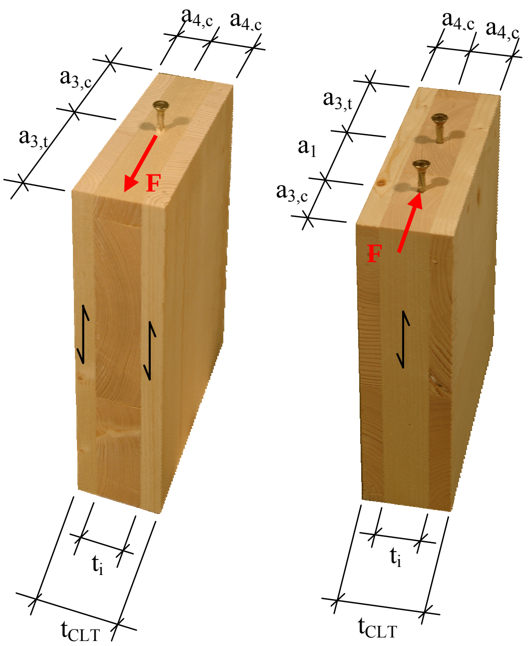

	Type of fastener	
	Self-tapping screws	Dowels
a_1	$10 \cdot d$	$4 \cdot d$
a_2	$3 \cdot d$	$4 \cdot d$
$a_{3,t}$	$12 \cdot d$	$5 \cdot d$
$a_{3,c}$	$7 \cdot d$	$3 \cdot d$
$a_{4,c}$	$5 \cdot d$	$3 \cdot d$

Fig. 14: Spacings, end distances and edge distances of fasteners in CLT

Table 5: Requirements for the geometry of edge joints in CLT with dowel type fasteners

Type of fastener	Minimum thickness of the relevant layer t_i in mm	Minimum thickness of CLT t_{CLT} in mm	Minimum thickness/ minimum embedded length $t_{1,req}$, $t_{2,req}$ in mm
Self-tapping screws	$d > 8$ mm: $3 \cdot d$ $d \leq 8$ mm: $2 \cdot d$	$10 \cdot d$	$10 \cdot d$
Dowels	d	$6 \cdot d$	$5 \cdot d$

4.2 Long-term tests

To examine the influence of load duration and climate variation on the load carrying capacity of edge joints with screws in CLT long-term tests were set up. The test programme contains 48 tests with axially loaded self-tapping screws driven into the middle layer of the test specimens parallel to the grain. The long-term behaviour of laterally loaded edge joints with self-tapping screws is also examined. To this purpose, tests with single and double shear CLT-to-CLT-connections are included in the test programme. The test set-up is documented in Fig. 15. The environmental conditions comply with Service Class 2. The design resistance of the test specimens was determined from the characteristic values with the modification factor $k_{mod} = 0{,}8$ and the partial factor $\gamma_M = 1{,}3$. The laterally loaded screws were loaded with the full design resistance while the axially loaded screws were loaded with 70 % of the design resistance. During the test duration the displacements are measured periodically and the climate is recorded. After three years the specimens will be unloaded and the remaining load carrying capacity will be determined in short-term tests.

Fig. 15: Long term tests with screwed edge joints in CLT under lateral load and axial load

5 Conclusions

For calculating the load carrying capacity of edge joints in CLT the parameters embedment strength and withdrawal capacity were examined. On the basis of statistical analysis of a multitude of test results it was possible to develop functions for predicted values of these parameters. Proposals for characteristic values are also given. The validity of the presented equations is limited to CLT with a characteristic density of 400 kg/m³ made of spruce. In tests with connections the required minimum edge and end distances and spacings of fasteners were determined. In addition the tests verify the calculation of the load carrying capacities. To determine the long-term behaviour of edge joints with self-tapping screws in CLT tests are performed.

6 References

[1] Blaß, H. J.; Uibel, T.: Tragfähigkeit von stiftförmigen Verbindungsmitteln in Brettsperrholz, *Karlsruher Berichte zum Ingenieurholzbau*, Band 8, Lehrstuhl für Ingenieurholzbau und Baukonstruktionen (Ed.), Universität Karlsruhe (TH), 2007

[2] Hilson, B. O. : Verbindungen mit stiftförmigen Verbindungsmitteln – Theorie. In: Blaß, H. J.; Görlacher, R.; Steck, G. (Ed.): *Holzbauwerke STEP1 – Bemessung und Baustoffe*, Fachverlag Holz, Düsseldorf, 1995

[3] Johansen, K. W.: Theory of timber connections. International Association of bridge and structural Engineering, Bern, 1949, p. 249-262

[4] Uibel, T.; Blaß, H. J.: Load carrying capacity of joints with dowel type fasteners in solid wood panels. In: Proceedings. CIB-W18 Meeting, Florence, Italy 2006, Paper 39-7-5

[5] EN 383: 1993 - Timber structures; Test methods; Determination of embedding strength and foundation values for dowel type fasteners

[6] EN 1382: 1999 - Timber structures - Test methods - Withdrawal capacity of timber fasteners